Medical & Biological Engineering & Computing (2022) 60:3169–3185
https://doi.org/10.1007/s11517-022-02661-6

ORIGINAL ARTICLE

On nonlinear dynamics of COVID-19 disease model corresponding to nonsingular fractional order derivative

Muhammad Arfan[1] · Maha M. A. Lashin[2] · Pongsakorn Sunthrayuth[3] · Kamal Shah[1,4] · Aman Ullah[1] · Kulpash Iskakova[5] · M. R. Gorji[6] · Thabet Abdeljawad[4,7]

Received: 30 December 2021 / Accepted: 15 June 2022 / Published online: 15 September 2022

Abstract
This manuscript is devoted to investigate the mathematical model of fractional-order dynamical system of the recent disease caused by Corona virus. The said disease is known as Corona virus infectious disease (COVID-19). Here we analyze the modified SEIR pandemic fractional order model under nonsingular kernel type derivative introduced by Atangana, Baleanu and Caputo ($\mathcal{ABC}$) to investigate the transmission dynamics. For the validity of the proposed model, we establish some qualitative results about existence and uniqueness of solution by using fixed point approach. Further for numerical interpretation and simulations, we utilize Adams-Bashforth method. For numerical investigations, we use some available clinical data of the Wuhan city of China, where the infection initially had been identified. The disease free and pandemic equilibrium points are computed to verify the stability analysis. Also we testify the proposed model through the available data of Pakistan. We also compare the simulated data with the reported real data to demonstrate validity of the numerical scheme and our analysis.

Keywords Non-integer order Adams-Bashforth technique · Approximate solution · COVID-19 model

1 Introduction

COVID-19 which is a threatful and terrible disease has been identified initially in Wuhan city of China in December 2019. The said infection transmitted in all over the world in coming few months. The spreading of this little and quickly transmissible virus in the recent time is due to corona virus [1, 2]. In 2020, the disease of COVID-19 is the world big threat that affected nearly all countries and continents around the globe. By the data given by the worldo-meter [3] and WHO [4, 5] shows that nearly 150 million cases of infection occurred while more than five million of population has been died. In the past history of the said virus, it is started in 1965 by the Tyrrell and Bynoe for identification of a virus

✉ Pongsakorn Sunthrayuth
pongsakorn_su@rmutt.ac.th

Muhammad Arfan
arfan_uom@yahoo.com

Maha M. A. Lashin
mmlashin@pnu.edu.sa

Kamal Shah
kamalshah408@gmail.com; kshah@psu.edu.sa

Aman Ullah
amanswt@gmail.com

Kulpash Iskakova
ahmanovakulpash@yahoo.com

M. R. Gorji
mohammad.rahimigorji@ugent.be; m69.rahimi@yahoo.com

Thabet Abdeljawad
tabdeljawad@psu.edu.sa

[1] Department of Mathematics, University of Malakand, Chakdara, Khyber Pakhtunkhwa, Pakistan

[2] Electrical Engineering Department, College of Engineering, Princess Nourah bint Abdulrahman University, P.O. Box 84428, Riyadh 11671, Saudi Arabia

[3] Department of Mathematics and Computer Science, Faculty of Science and Technology, Rajamangala University of Technology Thanyaburi (RMUTT), Thanyaburi, Pathumthani 12110, Thailand

[4] Department of Mathematics and Sciences, Prince Sultan University, Riyadh 11586, Saudi Arabia

[5] Department of Physics and Mathematics, Kazakh National Pedagogical University, Almaty, Kazakhstan

[6] Faculty of Medicine and Health Sciences, Ghent University, 9000 Ghent, Belgium

[7] Department of Medical Research, China Medical University, Taichung 40402, Taiwan

due to B814 [6]. Such types of viruses had been identified in human organs of embryonic tracheal organ moves taken from the respiration vain of an aged person [7].

Most of scientists, scholars and politicians are trying to stabilize and control the transmission of the pandemic, because the aforesaid disease has killed millions of people around the world in last 2 years. One of the factors of transmitting the said pandemic so rapidly is the migration of infectious population from one place to another. Therefore, locally and globally, some precautionary measures have been implemented. Most of the countries have stopped their air traffic and avoid unnecessary traveling [8]. They also banned crowds and lockdown in the cities to minimize the loss of human lives. In this scenario, the researchers and policies makers are searching to discover a cure or vaccine for the mention disease to stabilize and control it in the coming days. In preparation of vaccine some countries have got succession and now vaccines are available.

To properly controlled this pandemic, it is important to know much about the transmission, symptoms and features of this disease. Implementation of a proper method against the disease out breaking which is the big type of challenge faced by the human population in past history. Therefore, scientists and researchers are trying continuously to model this disease mathematically. In the past, different mathematical models have been developed for infectious diseases, for instance (see the references [9–15]). Recently, a lot of research work has been published in the form of mathematical models. For reference, we give for instance some published work as [1, 2, 16–22].

Most of mathematical models which have been investigated in the past were either the system of differential, difference and integration equation having natural or discrete-order. But after fractional calculus has got attention in last few decades, fractional order differential equations (FDEs) applied in excessive numbers to model various real-world problems. FDEs have many applications in various fields of engineering and medical laboratories like physics, business, controlling phenomena, accounting and in biological problems. Therefore, the scientists and researchers increasingly have used FDEs to formulate the real-globe phenomena. Because of the extra degree of choices in fractional derivative which is not present in traditional order operator. Further traditional order derivatives of integer order are not generalized as compared to fractional order which is generalized. Hence fractional order derivative is non-locale in nature and preserves the memory properties which makes it better. Further fractional order derivative of a function produces accumulation of the function which include the corresponding integer order counter part as a special case. Further geometrically it gives spectrum of the function and hence produce the whole density of the function on whom it applies. This is consider the best one, in the conditions where the coming states of models not only related to the present state but may also depend on the past timing of each quantity. For some significance applications see [23–26]. Due to these properties FDEs not only formulate the problems containing the non-Gaussian nature but can also describe the dynamics for the non-Markovian conditions also. As the natural order derivative and its constituting equations do not give knowledge lying between any of the two consecutive different natural numbers. Therefore, FDEs have been introduced to overcome these limitations. Fractional differential operators have many applications in different areas of mathematical and physical sciences. Liouville, Euler, Reimann and Fourier established some definitions for fractional order derivative during. After that the area has given much more attention. Modern calculus has a lot of applications in the area of mathematical modeling where hereditary characteristic and memorization properties have been studied very easily. Integer order derivative is rarely used to study such behaviors. Non-integer order derivative is the generalization of the natural order derivative having extra degree of freedom as compared the natural order derivative (see [23–30]). Keeping these properties scholars and researchers have taken much interest to study FDEs from different aspects. In the definition of arbitrary order operators, theirs lie a definite integration which predicts physically the area under the function curve or spectrum to generalize it. Integer order differentiation is a specific class of the non-integer order derivative. Although, sufficient contributions have been made by the researchers to analyze the solution of various problems (see [31–37]). Remarkably, arbitrary order operators have been formulated in different mathematical forms. Fractional differential operators can be classified in two major classes. One is devoted to singular kernel type fractional order differential operators like Reimann-Liouville, Caputo, etc. While the other class is devoted to non-singular type operator where exponential or Mittag-Leffler function play the role of kernel. One of the famous operator of fractional derivative with Mittag-Leffler type kernel is known as $\mathscr{ABC}$ introduced by Atangana, Baleanu and Caputo [38] in 2016. This operator replaced the singular kernel by non-singular one [39–41]. But this classification has own merits and de-merits. But researchers increasingly used these operators to investigate various real-world problems.

To treat FDEs under various operators for their numerical solution, optimization and numerical analysis, the traditional techniques have been extended for these purposes. For instance decomposition and homotopy perturbation techniques have been previously used to investigate various problems of FDEs (see [42–44]). For numerical solution mostly, RKM methods have been applied to various fractional order models. Here, in our work, the fractional Adams Bash-forth method is used for numerical simulation as applied in [45, 46]. This technique is an easy bi-step method which is more powerful than Taylor series, Euler method, and RKM techniques. Moreover, it is rapidly convergent and stable.

The investigation of epidemiological models of infected disease have gained great attention from research point of view. Several scholars have investigated the solution existence and uniqueness of many fractional order models [47–50]. For the

Table 1 Parameters description given in the model (1)

Notation	Parameters description
n_P	Birth rate
m_p	Infection death rate
b_p	rate of transmission
b_w	Disease transmission coefficient
ω_p, ω'_p	signified incubation period
γ_p, γ'_p	rate of recovered of I_p, A_p
ε, σ	Influence rate of virus from I_p and A_p to M
δ_p,	density of Asymptotic infectious population
κ	Multiplicity of transmissibility
ϑ	Eliminating rate of virus from M

description of the mathematical formulation of COVID-19, and to observe that how this disease impacts the susceptible, infected and quarantined people have been investigated. Some of the researchers have focused on the mathematical perspective of COVID-19. For knowing the dynamics structure and physical behavior of the outbreak of COVID-19, Mathematical models are playing important roles. In the problem presented in [51, 52] contains the susceptible people $S_p(t)$, exposed population $E_p(t)$, infectious density $I_p(t)$, asymptotically infectious people $A_p(t)$, humans recovery population $R_p(t)$, reservoir $M(t)$ and the their interactions have been modeled as

$$\begin{cases} \mathcal{D}_t(S_p(t)) = n_p - S_p m_p - b_p S_p(I_p + \kappa A_p) - b_w M S_p, \\ \mathcal{D}_t(E_p(t)) = (I_p + \kappa A_p) b_p S_p + b_w S_p M - \omega_p E_p(1-\delta_p) - \delta_p E_p \omega'_p - E_p m_p, \\ \mathcal{D}_t(I_p(t)) = \omega_p E_p(1-\delta_p) - I_p(\gamma_p + m_p), \\ \mathcal{D}_t(A_p(t)) = \delta_p \omega'_p E_p - (\gamma'_p + m_p) A_p, \\ \mathcal{D}_t(R_p(t)) = \gamma_p I_p + \gamma'_p A_p - m_p \gamma_p, \\ \mathcal{D}_t(M(t)) = \varepsilon I_p + \sigma A_p - \vartheta M, \\ S_p(0) = S_0,\ \ E_p(0) = E_0,\ \ I_p(0) = I_0,\ \ A_p(0) = A_0,\ \ R_p(0) = A_0,\ M(0) = M_0. \end{cases} \tag{1}$$

The detail of parameters applied in the problem (1), with full explanation is provided in Table 1.

Here authors have established some global, local stability by computing basic reproductive numbers. Also using simple integral transform method, they have presented some numerical results.

Motivated from the aforesaid literature and work published in the corresponding area, we consider Model (1) under the $\mathcal{ABC}$ fractional order derivative as

$$\begin{cases} {}^{ABC}\mathcal{D}_t^r(S_p(t)) = n_p - m_p S_p - b_p S_p(I_p + \kappa A_p) - b_w S_p M, \\ {}^{ABC}\mathcal{D}_t^r(E_p(t)) = (I_p + \kappa A_p) b_p S_p + b_w S_p M - \omega_p E_p(1-\delta_p) - \delta_p \omega'_p E_p - m_p E_p, \\ {}^{ABC}\mathcal{D}_t^r(I_p(t)) = \omega_p E_p(1-\delta_p) - I_p(\gamma_p + m_p), \\ {}^{ABC}\mathcal{D}_t^r(A_p(t)) = \delta_p \omega'_p E_p - (\gamma'_p + m_p) A_p, \\ {}^{ABC}\mathcal{D}_t^r(R_p(t)) = \gamma_p I_p + \gamma'_p A_p - m_p \gamma_p, \\ {}^{ABC}\mathcal{D}_t^r(M(t)) = \varepsilon I_p + \sigma A_p - \vartheta M, \\ S_p(0) = S_0,\ \ E_p(0) = E_0,\ \ I_p(0) = I_0,\ \ A_p(0) = A_0,\ \ R_p(0) = A_0, \\ M(0) = M_0,\ \ 0 < r \leq 1. \end{cases} \tag{2}$$

We establish some appropriate results for existence theory of solution via fixed point approach. Further, we attempt on stability results for the suggested model. Some sensitivity results about the parameters of the model are also discussed. Further, numerical technique of Adams-Bashforth method is used to handle this model (2) for the approximate solution and numerical simulations. Further we testify the numerical interpretation by two sets of data one of Wuhan city reported and other one is reported in about Pakistan. Further we also compared our simulated data and real data in case of infected cases to see the validity of the numerical scheme.

Here we remark some limitations of using mathematical models to understand the mechanism of infections disease or other real-world problems. For instance, models that establish for addressing forecasts are usually designed to produce either short-term or long-term forecasts. Some times models designed for long-term forecasting often do not produce good short-term forecasts and vice versa. Also, the associated factors, assumptions and structure, required for the one purpose often make the model less suitable for the other. To construct an appropriate model is a crucial job, because it is often the only link between the model and the model user. Also in majority cases to verify the model by real data, we often have no access to the afore data or information. In short we say that models are abstractions of reality, because, real-world systems are complex and composed of many interrelated components. For a modeler it is impossible or tedious to include all the comments (see detail in [57]). On the other hand for simulations, different numerical schemes are using to deal mathematical models. The concerned schemes have some short comings. For instance often numerical scheme is stable that we are using but on the other hands it will suffer from convergency. In same fashion it is not necessary that a scheme we use is convergent then it must also be stable. Here we use Adams-Bashforth method to simulate our results. The advantage of the proposed method is that it uses only one additional function evaluation per step and produces preserve high-order accuracy. But the limitation of the said method is the necessity of using another method to start.

2 Method, feasibility and stability analysis

Here in this part, we have to find feasibility and stability analysis of the proposed model. We first here re-collect some required results, definitions from [39, 40].

Definition 2.1 $\mathcal{ABC}$ fractional operator for a function $\Psi(t)$ and $\Psi(t) \in \mathcal{H}^1(0, \tau)$ is formulated as:

$$ {}^{ABC}\mathbf{D}_0^r\Psi(t) = \frac{ABC(r)}{1-r}\int_0^t \frac{d}{dz}\Psi(z)\kappa_r\left[\frac{-r}{1-r}\left(t-z\right)^r\right]dz. \tag{3}$$

If we change $\kappa_r\left[\frac{-r}{1-r}\left(t-z\right)^r\right]$ to $\kappa_1=\exp\left[\frac{-r}{1-r}\left(t-z\right)\right]$, in (3), then we will obtain the Caputo-Fabrizo (CF) operator of fractional orders. Further, it is to be noted that

$$^{ABC}\mathbf{D}^r[constant]=0.$$

$\mathcal{ABC}(r)$ is called normalized mapping as $\mathcal{ABC}(0)=\mathcal{ABC}(1)=1$. Also κ_r represents specific mapping known as Mittag-Leffler which is the general form of the exponential mapping [28–30].

Definition 2.2 Consider $\Psi\in L[0,T]$, then the fractional order integration in the sense of $\mathcal{ABC}$ is as follows:

$$^{ABC}\mathbf{I}_0^r\Psi(t)=\frac{1-r}{\mathcal{ABC}(r)}\Psi(t)+\frac{r}{\mathcal{ABC}(r)\Gamma(r)}\int_0^t(t-z)^{r-1}\Psi(z)dz. \quad (4)$$

Lemma 2.3 ([54]) If $Y(t)\to 0$ as $t=0$, then the solution for $0<r<1$ of the problem

$$\begin{aligned}^{ABC}\mathbf{D}_0^r\Psi(t)&=Y(t),\ t\in[0,T],\\ \Psi(0)&=\Psi_0\end{aligned}$$

is given by

$$\Psi(t)=\Psi_0+\frac{(1-r)}{\mathcal{ABC}(r)}Y(t)+\frac{r}{\Gamma(r)\mathcal{ABC}(r)}\int_0^t(t-z)^{r-1}Y(z)dz.$$

Note: For existence of solution, closed norm space is defined by:

$$\mathbf{Y}=\mathbf{Z}=C([0,T]\times R^6,R),$$

where $\mathbf{Z}=C[0,T]$ under the norm:

$$\|\mathbf{Y}\|=\|\Psi\|=\sup_{t\in[0,T]}\left[|S_p(t)|+|E_p(t)|+|I_p(t)|+|A_p(t)|+|R_p(t)|+|M(t)|\right].$$

The Krasnosilkii's theorem of fixed point theory is applied for the main result.

Theorem 2.4 [55] Consider $\mathbf{A}$ be any convexed subset of $\mathbf{Y}$ and consider that $\mathbf{F}$,$\mathbf{G}$ are two different operators in the integral equations with

1. $\mathbf{G}w+\mathbf{F}w\in\mathbf{A}$ for all $w\in\mathbf{A}$;
2. $\mathbf{F}$ is contracted operator;
3. $\mathbf{G}$ is compact and continuous operator.

Then equation $\mathbf{F}w+\mathbf{G}w=w$ in operator form, has one or more than one solution.

Lemma 2.5 The solution of the proposed problem (2) is bounded in the region of feasibility given by

$$\Psi=\left\{(S_p(t),E_p(t),I_p(t),A_p(t),R_p(t),M(t))\in\mathbf{R}_+^6\ :\ 0\le N(t)\le\frac{n_p}{m_p}\right\}.$$

Proof Let consider

$$N_p=S_p(t)+E_p(t)+I_p(t)+A_p(t)+R_p(t)+M(t).$$

By adding all the equations of (2) we get as

$$ll\frac{^{ABC}d^r(N_p)}{dt^r}\le n_p-m_pN_p. \quad (5)$$

Solving Eq. (5), we get

$$N_p\le\frac{n_p}{m_p}-C\exp(-m_pt),$$

or

$$N_p(t)\le\frac{n_p}{m_p},$$

hence proved.

Next we find the disease free and the pandemic equilibrium points by setting all the equation of system (2) equal zero as

$$\begin{aligned}^{ABC}\mathcal{D}_t^r(S_p(t))&=0,\\ ^{ABC}\mathcal{D}_t^r(E_p(t))&=0,\\ ^{ABC}\mathcal{D}_t^r(I_p(t))&=0,\\ ^{ABC}\mathcal{D}_t^r(A_p(t))&=0,\\ ^{ABC}\mathcal{D}_t^r(R_p(t))&=0,\\ ^{ABC}\mathcal{D}_t^r(M(t))&=0,\end{aligned}$$

or

$$E_0(\frac{n_p}{m_p},0,0,0,0,0).$$

Theorem 2.6 The basic reproductive number is computed as

$$R_0=\frac{\delta_p\omega_p'(m_p+\gamma_p)(\vartheta\kappa b_pn_p+n_p\delta b_w)+(1-\delta_p)\omega_p(\gamma_p'+m_p)(\vartheta b_pn_p+n_p\epsilon b_w)}{\vartheta m_p(m_p+\gamma_p)(\gamma_p'+m_p)(\delta_p(\omega_p'-\omega_p)+m_p+w_p)}$$

Proof For this we take the four equations of model (2) as

$$\frac{^{ABC}d^r(N_p)}{dt^r}=\begin{pmatrix}(I_p+\kappa A_p)b_pS_p+b_wS_pM-\omega_pE_p(1-\delta_p)-\delta_p\omega_p'E_p-m_pE_p\\ \omega_pE_p(1-\delta_p)-I_p(\gamma_p+m_p)\\ \delta_p\omega_p'E_p-(\gamma_p'+m_p)A_p\\ \epsilon I_p+\sigma A_p-\vartheta M\end{pmatrix}.$$

We define F and V as follows

$$F=\begin{pmatrix}(I_p+\kappa A_p)b_pS_p+b_wS_pM\\ 0\\ 0\\ 0\end{pmatrix}$$

and

$$V = \begin{pmatrix} \omega_p E_p(1-\delta_p) + \delta_p \omega'_p E_p + m_p E_p \\ \omega_p E_p(1-\delta_p) - I_p(\gamma_p + m_p) \\ \delta_p \omega'_p E_p - (\gamma'_p + m_p)A_p \\ \varepsilon I_p + \sigma A_p - \vartheta M \end{pmatrix}.$$

Next, taking the Jacobian of F and V w.r.t. t, and putting the value of E_0, we get

$$\mathcal{F} = \begin{pmatrix} 0 & \frac{b_p n_p}{m_p} & \frac{\kappa b_p n_p}{m_p} & \frac{b_w n_p}{m_p} \\ 0 & 0 & 0 & 0 \\ 0 & 0 & 0 & 0 \\ 0 & 0 & 0 & 0 \end{pmatrix}$$

and

$$\mathcal{V} = \begin{pmatrix} \delta_p \omega'_p + \omega_p(1-\delta_p) + m_p & 0 & 0 & 0 \\ \omega_p(\delta_p - 1) & m_p + \gamma_p & 0 & 0 \\ -\delta_p \omega'_p & 0 & \gamma'_p + m_p & 0 \\ 0 & -\varepsilon_p & -\delta & \vartheta \end{pmatrix}.$$

Then the dominant eigen value of $\mathcal{F}\mathcal{V}^{-1} = \rho(\mathcal{F}\mathcal{V}^{-1})$ is called basic reproduction number R_0 and hence equal to

$$R_0 = \frac{\delta_p \omega'_p (m_p+\gamma_p)(\vartheta \kappa b_p n_p + n_p \delta b_w) + (1-\delta_p)\omega_p(\gamma'_p + m_p)(\vartheta b_p n_p + n_p \varepsilon b_w)}{\vartheta m_p (m_p+\gamma_p)(\gamma'_p + m_p)(\delta_p(\omega'_p - \omega_p) + m_p + w_p)}. \quad (6)$$

Hence proved

Theorem 2.7 E_0 is locally asymptotically stable if $R_0 < 1$.

Proof The derivation of the theorem can be obtained by taking Jacobian of the system (2) and putting $E_0 = (\frac{n_p}{m_p}, 0, 0, 0, 0, 0)$, one has

$$\mathcal{J} = \begin{pmatrix} -m_p & 0 & \frac{-b_p n_p}{m_p} & \frac{-\kappa b_p n_p}{m_p} & 0 & \frac{-b_w n_p}{m_p} \\ 0 & -m_p - \delta_p \omega'_p - (1-\delta_p)\omega_p & \frac{b_p n_p}{m_p} & \frac{\kappa b_p n_p}{m_p} & 0 & \frac{b_w n_p}{m_p} \\ 0 & (1-\delta_p)\omega_p & -m_p - \gamma_p & 0 & 0 & 0 \\ 0 & \delta_p \omega'_p & 0 & -m_p - \gamma'_p & 0 & 0 \\ 0 & 0 & \gamma_p & \gamma'_p & -m_p & 0 \\ 0 & 0 & \varepsilon & \delta & 0 & -\vartheta \end{pmatrix}.$$

In the above matrix, two of the eigen values on the main diagonal are negative, while the rest of the eigen values can be computed by characteristic equation as

$$\Lambda^4 + b_1 \Lambda^3 + b_2 \Lambda^2 + b_3 \Lambda + b_4 = 0. \quad (7)$$

Here

$$\begin{aligned} b_1 &= \gamma'_p + \delta + \delta_p \omega'_p + (1-\delta_p)\omega_p + 3m_p + \gamma_p, \\ b_2 &= \underbrace{(m_p+\gamma_p)(\delta_p \omega'_p + (1-\delta_p)\omega_p + m_p) - b_p(1-\delta_p)\omega_p} \\ &+ \underbrace{(m_p+\gamma_p)(\delta_p(\omega'_p - \omega_p) + m_p - \omega_p) - \kappa b_p \delta_p \omega'_p} \\ &+ \vartheta(\gamma'_p + m_p) + (m_p+\gamma_p)(m_p+\gamma'_p) + \vartheta(\delta_p(\omega'_p - \omega_p) + m_p + \omega_p) + \vartheta(m_p+\gamma_p), \\ b_3 &= \vartheta(\delta_p \omega'_p + (1-\delta_p)\omega_p + m_p)[(\gamma'_p + m_p)(1-R_1) + (m_p+\gamma_p)(1-R_2)] \\ &+ (m_p+\gamma_p)\underbrace{(\delta(\gamma'_p + m_p) - (\kappa b_p \delta_p \omega'_p))} + b_p \delta_p \omega_p (\gamma'_p + m_p) \\ &+ (\gamma'_p + m_p)((\gamma_p + m_p)\delta_p(\omega'_p - \omega_p) + m_p + \omega_p) - b_p \omega_p, \\ b_4 &= \vartheta(\gamma_p + m_p)(\gamma'_p + m_p)(\delta + \delta_p \omega'_p + (1-\delta_p)\omega_p + m_p)(1-R_0), \end{aligned}$$

where $R_0 = R_1 + R_2$ as follows

$$R_1 = \frac{\delta_p \omega'_p (\vartheta \kappa b_p n_p + n_p \delta b_w)}{\vartheta m_p (\gamma'_p + m_p)(\delta_p(\omega'_p - \omega_p) + m_p + w_p)}$$

and

$$R_2 = \frac{(1-\delta_p)\omega_p(\gamma_p + m_p)(\vartheta b_p n_p + n_p \varepsilon b_w)}{\vartheta m_p (\gamma_p + m_p)(\delta_p(\omega'_p - \omega_p) + m_p + w_p)}.$$

In the above characteristic equation, the terms which are underlines are less than R_0, also b_4 is positive if $R_0 < 1$. Further if $R_1 < 1$ and $R_2 < 1$, then b_3 will be positive. Hence all the coefficients are positive being the conditions for Routh-Hurwitz criteria [53]. Hence E_0 is locally asymptotically stable.

Next we have to find the pandemic equilibrium point as

$$E^* = (S^*_P, E^*_P, I^*_P, A^*_P, R^*_P, M^*)$$

and

$$\begin{aligned} S^*_p &= \frac{n_p}{\Lambda + m_p}, \\ E^*_p &= \frac{\Lambda S^*_p}{\delta_p \omega'_p - \delta_p \omega_p + m_p + \omega_p}, \\ I^*_p &= \frac{E^*_P(1-\delta_p)\omega_p}{\gamma_p + m_p}, \\ A^*_P &= \frac{E^*_p \delta_p \omega'_p}{\gamma'_p + m_p}, \\ R^*_P &= \frac{A^*_p \gamma'_p + I^*_p \gamma_p}{+m_p}, \\ M^* &= \frac{A^*_p \delta + I^*_p \varepsilon}{\vartheta}. \end{aligned}$$

Here

$$\Lambda = \frac{b_p(\kappa n_p A^*_p + m_p I^*_p)}{m_p(S^*_p + E^*_p + I^*_p + A^*_p + R^*_p)} + \frac{b_p M^*}{m_p},$$

satisfying the given equation

$$P(\Lambda^*) = a_1(\Lambda^*)2 + a_2(\Lambda^*) = 0.$$

Here

$$a_1 = \vartheta(m_p + \gamma_p)(m_p + \gamma'_p)(\delta_p(\omega'_p - \omega_p) + m_p + \omega_p)$$

$$a_2 = \vartheta m_p(m_p + \gamma_p)(m_p + \gamma'_p)(\delta_p(\omega'_p - \omega_p) + m_p + \omega_p)(1 - R_0)$$

As $a1 > 0, a_2 \geq 0$ if $R_0 < 1$, then $\Lambda^* = \frac{-a_2}{a_1} \leq 0$. Hence no pandemic equilibrium will lie if $R_0 \leq 1$. This implies that the endemic equilibrium exists and stable if $R_0 > 1$.

3 Existence, uniqueness of solution and numerical simulations

It is natural to ask whether a dynamical system that we are investigating exists or not in reality. Fixed point theory answer this question. We examine our considered problem (2) for existence results about the solution. Regarding this, we write the right sides of our problem (2) as:

$$\begin{cases} \mathrm{F}_1(t, S_p, E_p, I_p, A_p, R_p, M) = n_p - S_p m_p - b_p S_p(I_p + \kappa A_p) - S_p M b_w, \\ \mathrm{F}_2(t, S_p, E_p, I_p, A_p, R_p, M) = (I_p + \kappa A_p) b_p S_p + b_w S_p M - (1-\delta_p)\omega_p E_p - E_p \delta_p \omega'_p - E_p m_p, \\ \mathrm{F}_3(t, S_p, E_p, I_p, A_p, R_p, M) = (1-\delta_p)\omega_p E_p - (\gamma_p + m_p) I_p, \\ \mathrm{F}_4(t, S_p, E_p, I_p, A_p, R_p, M) = \delta_p \omega'_p E_p - (\gamma'_p + m_p) A_p, \\ \mathrm{F}_5(t, S_p, E_p, I_p, A_p, R_p, M) = \gamma_p I_p + \gamma'_p A_p - m_p \gamma_p, \\ \mathrm{F}_6(t, S_p, E_p, I_p, A_p, R_p, M) = \varepsilon I_p + \sigma A_p - \vartheta M, \\ S_p(0) = S_0,\ E_p(0) = E_0,\ I_p(0) = I_0,\ A_p(0) = A_0,\ R_p(0) = A_0,\ M(0) = M_0. \end{cases} \tag{8}$$

To symbolize the system (2) by using (8) as follows

$$\begin{aligned} {}^{\mathcal{ABC}}\mathbf{D}^r_{+0}\mathcal{Y}(t) &= \Omega(t, \mathcal{Y}(t)),\ t \in [0, \tau],\ 0 < r \leq 1, \\ \mathcal{Y}(0) &= \mathcal{Y}_0. \end{aligned} \tag{9}$$

By applying integral in sense of $\mathcal{ABC}$ and by using lemma 2.3 we get

$$\mathcal{Y}(t) = \mathcal{Y}_0(t) + \frac{(1-r)}{\mathcal{ABC}(r)}\left[\Omega(t, \mathcal{Y}(t))\right] + \frac{r}{\mathcal{ABC}(r)\Gamma(r)}\int_0^t (t-z)^{r-1}\Omega(z, \mathcal{Y}(z))dz, \tag{10}$$

where,

$$\mathcal{Y}(t) = \begin{cases} S_p(t) \\ E_p(t) \\ I_p(t) \\ A_p(t) \\ R_p(t) \\ M(t) \end{cases},\quad \mathcal{Y}_0(t) = \begin{cases} S_0 \\ E_0 \\ I_0 \\ A_0 \\ R_0 \\ M_0 \end{cases},\quad \Omega(t, \mathcal{Y}(t)) = \begin{cases} \mathrm{F}_1(S_p, E_p, I_p, A_p, R_p, M, t) \\ \mathrm{F}_2(t, S_p, E_p, I_p, A_p, R_p, M) \\ \mathrm{F}_3(t, S_p, E_p, I_p, A_p, R_p, M) \\ \mathrm{F}_4(t, S_p, E_p, I_p, A_p, R_p, M) \\ \mathrm{F}_5(t, S_p, E_p, I_p, A_p, R_p, M) \\ \mathrm{F}_6(t, S_p, E_p, I_p, A_p, R_p, M). \end{cases} \tag{11}$$

Using (9) and define operators $\mathbf{F}$,$\mathbf{G}$ by using (10) as

$$\begin{aligned} \mathbf{F}(\mathcal{Y}) &= \mathcal{Y}_0(t) + \tfrac{(1-r)}{\mathcal{ABC}(r)}\left[\Omega(t, \mathcal{W}(t))\right], \\ \mathbf{G}(\mathcal{Y}) &= \tfrac{r}{\Gamma(r)\mathcal{ABC}(r)}\int_0^t (t-z)^{r-1}\Omega(Z, \mathcal{Y}(z))dz. \end{aligned} \tag{12}$$

Witting the growth condition and Lipschitz condition for solution's existence and uniqueness as given below.

(B1) Let we have a constants A_Ω,E_Ω, as:

$$|\Omega(t, \mathcal{Y}(t))| \leq A_\Omega|\mathcal{Y}| + E_\Omega.$$

(B2) Let we have a constants $L_\Omega > 0$, as for all $\mathcal{Y}$, $\bar{Y} \in \mathbf{Y}$ as:

$$|\Omega(t, \mathcal{Y}) - \Omega(t, \bar{Y})| \leq L_\Omega[|\mathcal{Y}| - \bar{Y}|].$$

Theorem 3.1 Under hypothesis ($B1$,$B2$), the problem (10) has at least one solution which implies that the proposed model (2) has at least one solution if $\frac{(1-r)}{\mathcal{ABC}(r)}L_\Omega < 1$.

Proof The theorem can be proved by using the following two steps.

Step I: Consider $\bar{Y} \in \mathbf{B}$ and $\mathbf{B} = \{\mathcal{Y} \in \mathbf{Y} : \ \|\mathcal{Y}\| \leq \sigma, \sigma > 0\}$ is convex and close set. Then by $\mathbf{F}$ in (12), we obtain

$$\begin{aligned} \|\mathbf{F}(\mathcal{Y}) - \mathbf{F}(\bar{Y})\| &= \tfrac{(1-r)}{\mathcal{ABC}(r)}\max_{t\in[0,\tau]}\left|\Omega(t, \mathcal{Y}(t)) - \Omega(t, \bar{Y}(t))\right| \\ &\leq \tfrac{(1-r)}{\mathcal{ABC}(r)}L_\Omega\|\mathcal{Y} - \bar{Y}\|. \end{aligned} \tag{13}$$

Hence, $\mathbf{F}$ is contracted.

Step-II: To show that $\mathbf{G}$ is compact relative, it is enough to show that $\mathbf{G}$ is bounded and equi-continuous. Clearly, $\mathbf{G}$ is defined on their domain as Ω is defined on domain and for any $\mathcal{Y} \in \mathbf{B}$, we follow

$$\begin{aligned} \|\mathbf{G}(\mathcal{Y})\| &= \max_{t\in[0,\tau]}\|\tfrac{r}{\mathcal{ABC}(r)\Gamma(r)}\int_0^t (t-z)^{r-1}\Omega(z, \mathcal{Y}(z))dz\| \\ &\leq \tfrac{r}{\mathcal{ABC}(r)\Gamma(r)}\int_0^\tau (\tau-z)^{r-1}|\Omega(z, \mathcal{Y}(z))|dz \\ &\leq \tfrac{\tau^r}{\mathcal{ABC}(r)\Gamma(r)}[A_\Omega\sigma + E_\Omega]. \end{aligned} \tag{14}$$

So, from (14) it is clear that $\mathbf{G}$ have bounds. Further, for equi-continuous let $t_1 > t_2 \in [0,\tau]$, we continue as

$$\begin{aligned} |\mathbf{G}(\mathcal{Y}(t_2) - \mathbf{G}(\mathcal{Y}(t_1)| &= \tfrac{r}{\mathcal{ABC}(r)\Gamma(r)}\left|\int_0^{t_2}(t_2-z)^{r-1}\Omega(z, \mathcal{Y}(z))dz - \int_0^{t_1}(t_1-z)^{r-1}\Omega(z, \mathcal{Y}(z))dz\right| \\ &\leq \tfrac{[A_\Omega\sigma + E_\Omega]}{\mathcal{ABC}(r)\Gamma(r)}[t_2^r - t_1^r]. \end{aligned} \tag{15}$$

Equation (15) implies that as $t_2 \to t_1$ then the right side will approaches to zero. As, $\mathbf{G}$ is continuous and hence

$$|\mathbf{G}(\mathcal{Y}(t_2) - \mathbf{G}(\mathcal{Y}(t_1)| \to 0,\ \text{as } t_2 \to t_1.$$

Hence as $\mathbf{G}$ have bounds and are continuous so

$$\|\mathbf{G}(\mathcal{Y}(t_2) - \mathbf{G}(\mathcal{Y}(t_1)\| \to 0,\ \text{as } t_2 \to t_1.$$

Thus, $\mathbf{G}$ have bounds and equi-continuous operator. Also, from theorem of Arzelá-Ascoli, the operator $\mathbf{G}$ is relative compact and hence continuous completely. Thus, from Theorem 3.1, the integration Equation (10) has Als at least one solution and therefore the proposed problem has at least one solution.

For unique solution we give the given theorem.

Theorem 3.2 By hypothesis ($B2$), the integral Equation (10) has unique solution which yields that the system under consideration (2) has unique solution if:

$$\left[\frac{(1-r)L_\Omega}{\mathcal{ABC}(r)} + \frac{\tau^r L_\Omega}{\mathcal{ABC}(r)\Gamma(r)}\right] < 1.$$

Proof Consider the mapping $\mathbf{T}:\mathbf{Y}\to\mathbf{Y}$ defined by

$$\begin{aligned}\mathbf{T}\mathcal{Y}(t) &= \mathcal{Y}_0(t) + \left[\Omega(t,\mathcal{Y}(t)) - \Omega_0(t)\right]\frac{(1-r)}{\mathcal{ABC}(r)}\\ &\quad + \frac{r}{\mathcal{ABC}(r)\Gamma(r)}\int_0^t (t-z)^{r-1}\Omega(z,\mathcal{Y}(z))dz,\ t\in[0,\tau].\end{aligned} \tag{16}$$

Let $\mathcal{Y}, \bar{Y} \in \mathbf{Y}$, then one can take

$$\begin{aligned}\|\mathbf{T}\mathcal{Y} - \mathbf{T}\bar{Y}\| &\le \frac{(1-r)}{\mathcal{ABC}(r)}\max_{t\in[0,\tau]}\left|\Omega(t,\mathcal{Y}(t)) - \Omega(t,\bar{Y}(t))\right|\\ &+ \frac{r}{\mathcal{ABC}(r)\Gamma(r)}\max_{t\in[0,\tau]}\left|\int_0^t (t-z)^{r-1}\Omega(z,\mathcal{Y}(z))dz - \int_0^t (t-z)^{r-1}\Omega(z,\bar{Y}(z))dz\right|\\ &\le \Upsilon\|\mathcal{Y} - \bar{Y}\|,\end{aligned} \tag{17}$$

where

$$\Upsilon = \left[\frac{(1-r)L_\Omega}{\mathcal{ABC}(r)} + \frac{\tau^r L_\Omega}{\mathcal{ABC}(r)\Gamma(r)}\right]. \tag{18}$$

Hence, $\mathbf{T}$ is contracted from (17). So, the integration Equation (10) has one root. This implies that the problem (2) has one solution.

For approximate solution, we continue this part of manuscript to the proposed fractional order (2) model in sense of ABC operator. The iterative technique are then simulated on different fractional orders. For this, we use the arbitrary order AB iterative technique [56] to find the numerical scheme for the graphical representation of the problem (2). For model (8) we develop a numerical scheme as

$$\begin{cases} {}^{\mathcal{ABC}}\mathcal{D}_t^r(S_p(t)) = \mathrm{F}_1(S_p(t),t) = n_p - m_pS_p - b_pS_p(I_p + \kappa A_p) - b_wS_pM,\\ {}^{\mathcal{ABC}}\mathcal{D}_t^r(E_p(t)) = \mathrm{F}_2(E_p(t),t) = (I_p + \kappa A_p)b_pS_p + b_wS_pM - \omega_pE_p(1-\delta_p) - \delta_p\omega'_pE_p - E_pm_p,\\ {}^{\mathcal{ABC}}\mathcal{D}_t^r(I_p(t)) = \mathrm{F}_3(I_p(t),t) = \omega_pE_p(1-\delta_p) - I_p(\gamma_p + m_p),\\ {}^{\mathcal{ABC}}\mathcal{D}_t^r(A_p(t)) = \mathrm{F}_4(A_p(t),t) = \delta_p\omega'_pE_p - (\gamma'_p + m_p)A_p,\\ {}^{\mathcal{ABC}}\mathcal{D}_t^r(R_p(t)) = \mathrm{F}_5(R_p(t),t) = \gamma_pI_p + \gamma'_pA_p - m_p\gamma_p,\\ {}^{\mathcal{ABC}}\mathcal{D}_t^r(M(t)) = \mathrm{F}_6(M(t),t) = \varepsilon I_p + \sigma A_p - \vartheta M,\\ S_p(0) = S_0,\ E_p(0) = E_0,\ I_p(0) = I_0,\ A_p(0) = A_0,\ R_p(0) = A_0,\ M(0) = M_0. \end{cases} \tag{19}$$

Integrating first equation of (19) in $\mathcal{ABC}$ approach, we get

$$S_p(t) - S_p(0) = \frac{(1-r)}{\mathcal{ABC}(r)}\left[\mathrm{F}_1(S_p(t),t)\right] + \frac{r}{\mathcal{ABC}(r)\Gamma(r)}\int_0^t (t-z)^{r-1}\mathrm{F}_1(S_p(z),z)dz.$$

Consider $t = t_{i+1}$ for $i = 0,1,2\cdots$, it follows that

$$\begin{aligned}S_p(t_{i+1}) - S_p(0) &= \frac{(1-r)}{\mathcal{ABC}(r)}\left[\mathrm{F}_1(S_p(t_i),t_i)\right]\\ &\quad + \frac{r}{\mathcal{ABC}(r)\Gamma(r)}\int_0^{t_{i+1}}(t_{i+1}-z)^{r-1}\mathrm{F}_1(S_p(z),z)dz,\\ &= \frac{(1-r)}{\mathcal{ABC}(r)}\left[\mathrm{F}_1(S_p(t_i),t_i)\right]\\ &\quad + \frac{r}{\mathcal{ABC}(r)\Gamma(r)}\sum_{q=0}^{i}\int_q^{t_{q+1}}(t_{i+1}-z)^{r-1}\mathrm{F}_1(S_p(z),z)dz.\end{aligned}$$

Next, approximating the mapping $F_1(S_p(t),t)$ on time interval $[t_q,t_{q+1}]$, by the interpolating expression as follows:

$$F_1(S_p(t),t) \cong \frac{F_1(S_p(t_q),t_q)}{\Delta}(t - t_{q-1}) + \frac{F_1(S_p(t_{q-1}),t_{q-1})}{\Delta}(t - t_q)$$

or

$$\begin{aligned}S_p(t_{i+1}) &= S_p(0) + \frac{(1-r)}{\mathcal{ABC}(r)}\left[\mathrm{F}_1(S_p(t_i),t_i)\right]\\ &\quad + \frac{r}{\mathcal{ABC}(r)\Gamma(r)}\sum_{q=0}^{i}\left(\frac{F_1(S_p(t_q),t_q)}{\Delta}\int_q^{t_{q+1}}(t-t_{q-1})(t_{i+1}-t)^{r-1}dt\right.\\ &\quad \left. - \frac{F_1(S_p(t_{q-1}),t_{q-1})}{\Delta}\int_q^{t_{q+1}}(t-t_q)(t_{i+1}-t)^{r-1}dt\right)\\ &= S_p(0) + \frac{(1-r)}{\mathcal{ABC}(r)}\left[\mathrm{F}_1(S_p(t_i),t_i)\right]\\ &\quad + \frac{r}{\mathcal{ABC}(r)\Gamma(r)}\sum_{q=0}^{i}\left(\frac{F_1(S_p(t_q),t_q)}{\Delta}I_{q-1,r} - \frac{F_1(S_p(t_{q-1}),t_{q-1})}{\Delta}I_{q,r}\right).\end{aligned} \tag{20}$$

Now the integrals $I_{q-1,r}$ and $I_{q,r}$ can be calculated as follow:

$$\begin{aligned}I_{q-1,r} &= \int_q^{t_{q+1}}(t-t_{q-1})(t_{i+1}-t)^{r-1}dt\\ &= -\frac{1}{r}\left[(t_{q+1}-t_{q-1})(t_{i+1}-t_{q+1})^r - (t_q - t_{q-1})(t_{i+1}-t_q)^r\right]\\ &\quad - \frac{1}{r(r-1)}\left[(t_{i+1}-t_{q+1})^{r+1} - (t_{i+1}-t_q)^{r+1}\right],\end{aligned}$$

and

$$\begin{aligned}I_{q,r} &= \int_q^{t_{q+1}}(t-t_q)(t_{i+1}-t)^{r-1}dt\\ &= -\frac{1}{r}\left[(t_{q+1}-t_q)(t_{i+1}-t_{q+1})^r\right]\\ &\quad - \frac{1}{r(r-1)}\left[(t_{i+1}-t_{q+1})^{r+1} - (t_{i+1}-t_q)^{r+1}\right],\end{aligned}$$

put $t_q = q\Delta$, we get

Table 2 Description of the parameters given in model (1) for Wuhan

Notation	Numerical value
n_P	0.073
m_p	0.00408
b_p	0.05
b_w	0.000001231
ω_p, ω'_p	0.1243, 0.005
γ_p, γ'_p	0.09871, 0.854302
ε, σ	0.1243, 0.01
ϑ	0.398
δ_p,	0.1243
κ	0.02

$$\begin{aligned} I_{q-1,r} &= -\tfrac{\Delta^{r+1}}{r}\Big[(q+1-(q-1))(i+1-(q+1))^r-(q-(q-1))(i+1-q)^r\Big] \\ &\quad -\tfrac{\Delta^{r+1}}{r(r-1)}\Big[(i+1-(q+1))^{r+1}-(i+1-q)^{r+1}\Big], \\ &= \tfrac{\Delta^{r+1}}{r(r-1)}\Big[-2(r+1)(i-q)^r+(r+1)(i+1-q)^r-(i-q)^{r+1}+(i+1-q)^{r+1}\Big], \\ &= \tfrac{\Delta^{r+1}}{r(r-1)}\Big[(i-q)^r(-2(r+1)-(i-q))+(i+1-q)^r(r+1+i+1-q)\Big], \\ &= \tfrac{\Delta^{r+1}}{r(r-1)}\Big[(i+1-q)^r(i-q+2+r)-(i-q)^r(i-q+2+2r)\Big], \end{aligned} \tag{21}$$

and

$$\begin{aligned} I_{q,r} &= -\tfrac{\Delta^{r+1}}{r}\Big[(q+1-q)(i+1-(q+1))^r\Big]-\tfrac{\Delta^{r+1}}{r(r-1)}\Big[(i+1-(q+1))^{r+1}-(i+1-q)^{r+1}\Big], \\ &= \tfrac{\Delta^{r+1}}{r(r-1)}\Big[-(r+1)(i-q)^r-(i-q)^{r+1}+(i+1-q)^{r+1}\Big], \\ &= \tfrac{\Delta^{r+1}}{r(r-1)}\Big[(i-q)^r(-(r+1)-(i-q))+(i+1-q)^{r+1}\Big], \\ &= \tfrac{\Delta^{r+1}}{r(r-1)}\Big[(i+1-q)^{r+1}-(i-q)^r(i-q+1+r)\Big], \end{aligned} \tag{22}$$

substitute (21) and (22) in (20), we get

$$\begin{aligned} S_p(t_{i+1}) &= S_p(0)+\tfrac{(1-r)}{ABC(r)}\Big[\mathrm{F}_1(S_p(t_i),t_i)\Big] \\ &\quad +\tfrac{r}{ABC(r)}\sum_{q=0}^{i}\Bigg(\tfrac{F_1(S_p(t_q),t_q)}{\Gamma(r+2)}\Delta^r\Big[(i+1-q)^r(i-q+2+r) \\ &\quad -(i-q)^r(i-q+2+2r)\Big] \\ &\quad -\tfrac{F_1(S_p(t_{q-1}),t_{q-1})}{\Gamma(r+2)}\Delta^r[(i+1-q)^{r+1}-(i-q)^r(i-q+1+r)]\Bigg). \end{aligned}$$

Similarly, the proposed method can be used for the remaining five equations of (19) to form general algorithms as

$$\begin{aligned} E_p(t_{i+1}) &= E_p(0)+\tfrac{(1-r)}{ABC(r)}\Big[\mathrm{F}_2(E_p(t_i),t_i)\Big] \\ &\quad +\tfrac{r}{ABC(r)}\sum_{q=0}^{i}\Bigg(\tfrac{F_2(E_p(t_q),t_q)}{\Gamma(r+2)}\Delta^r\Big[(i+1-q)^r(i-q+2+r) \\ &\quad -(i-q)^r(i-q+2+2r)\Big] \\ &\quad -\tfrac{F_2(E_p(t_{q-1}),t_{q-1})}{\Gamma(r+2)}\Delta^r[(i+1-q)^{r+1}-(i-q)^r(i-q+1+r)]\Bigg). \end{aligned}$$

$$\begin{aligned} I_p(t_{i+1}) &= I_p(0)+\tfrac{(1-r)}{ABC(r)}\Big[\mathrm{F}_3(I_p(t_i),t_i)\Big] \\ &\quad +\tfrac{r}{ABC(r)}\sum_{q=0}^{i}\Bigg(\tfrac{F_3(I_p(t_q),t_q)}{\Gamma(r+2)}\Delta^r\Big[(i+1-q)^r(i-q+2+r) \\ &\quad -(i-q)^r(i-q+2+2r)\Big] \\ &\quad -\tfrac{F_3(I_p(t_{q-1}),t_{q-1})}{\Gamma(r+2)}\Delta^r[(i+1-q)^{r+1}-(i-q)^r(i-q+1+r)]\Bigg). \end{aligned}$$

$$\begin{aligned} A_p(t_{i+1}) &= A_p(0)+\tfrac{(1-r)}{ABC(r)}\Big[\mathrm{F}_4(A_p(t_i),t_i)\Big] \\ &\quad +\tfrac{r}{ABC(r)}\sum_{q=0}^{i}\Bigg(\tfrac{F_4(A_p(t_q),t_q)}{\Gamma(r+2)}\Delta^r\Big[(i+1-q)^r(i-q+2+r) \\ &\quad -(i-q)^r(i-q+2+2r)\Big] \\ &\quad -\tfrac{F_4(A_p(t_{q-1}),t_{q-1})}{\Gamma(r+2)}\Delta^r[(i+1-q)^{r+1}-(i-q)^r(i-q+1+r)]\Bigg). \end{aligned}$$

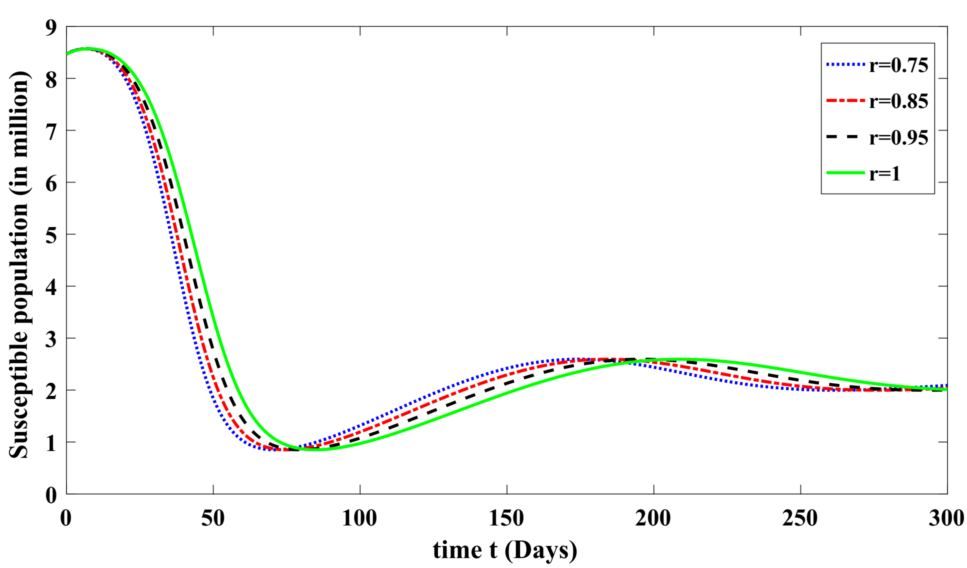

Fig. 1 Behavior of Susceptible population $S_p(t)$ at various arbitrary order r of the proposed system (2) for $h = 0.1, b_p = 0.05$

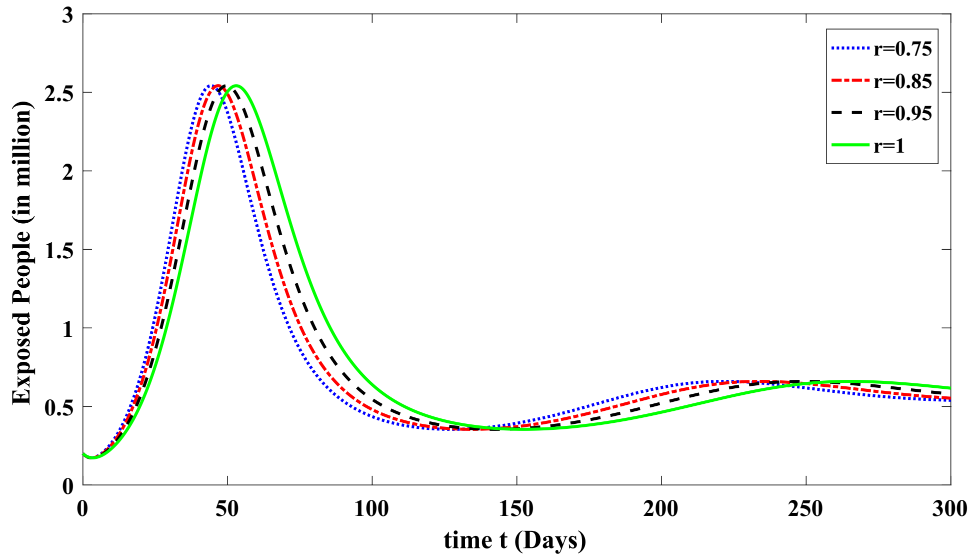

Fig. 2 Behavior of Exposed individuals $E_p(t)$ at various arbitrary order r of the proposed system (2) for $h = 0.1, b_p = 0.05$

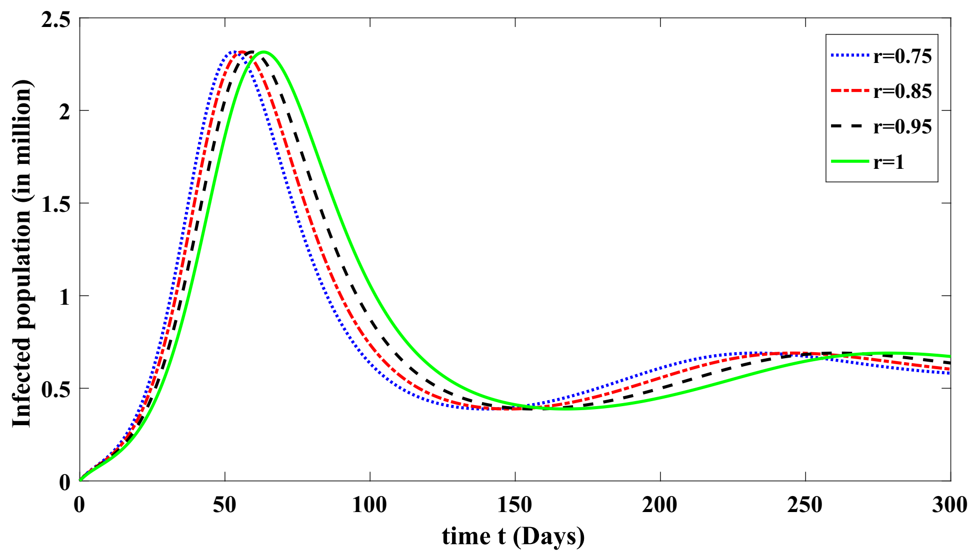

Fig. 3 Behavior of total infected population $I_p(t)$ at various arbitrary order r of the proposed system (2) for $h = 0.1, b_p = 0.05$

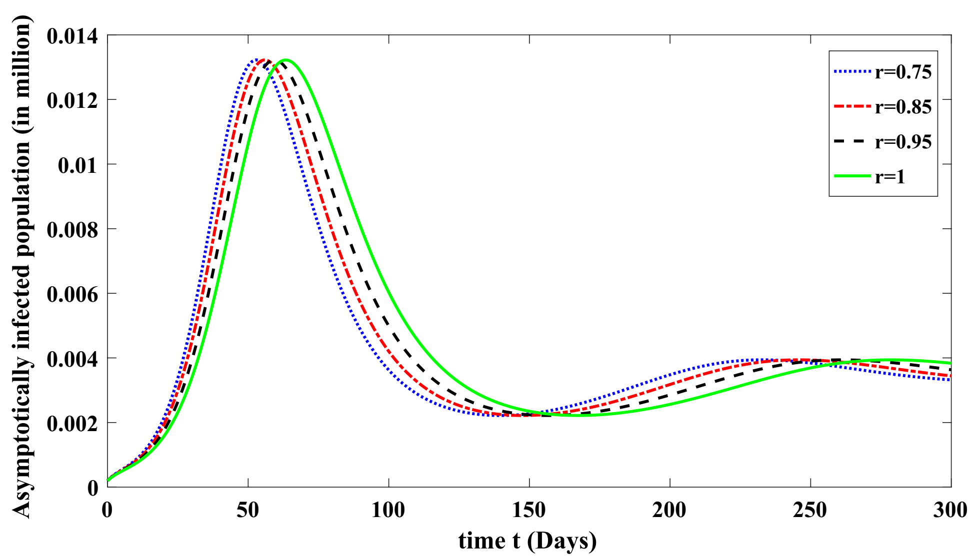

Fig. 4 Behavior of asymptotically infectious population $A_p(t)$ at various arbitrary order r of the proposed system (2) for $h = 0.1, b_p = 0.05$

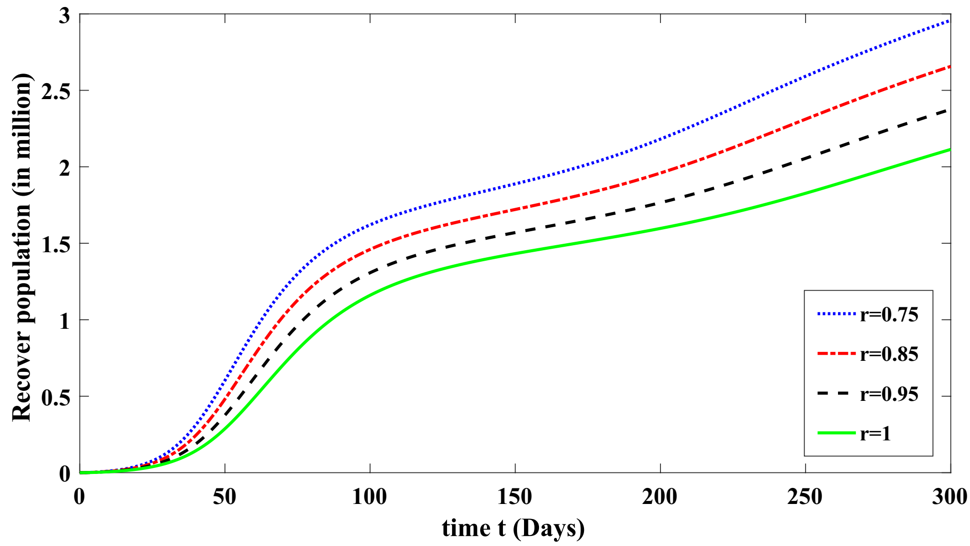

Fig. 5 Behavior of recovered population $R_p(t)$ at various arbitrary order r of the proposed system (2) for $h = 0.1, b_p = 0.05$

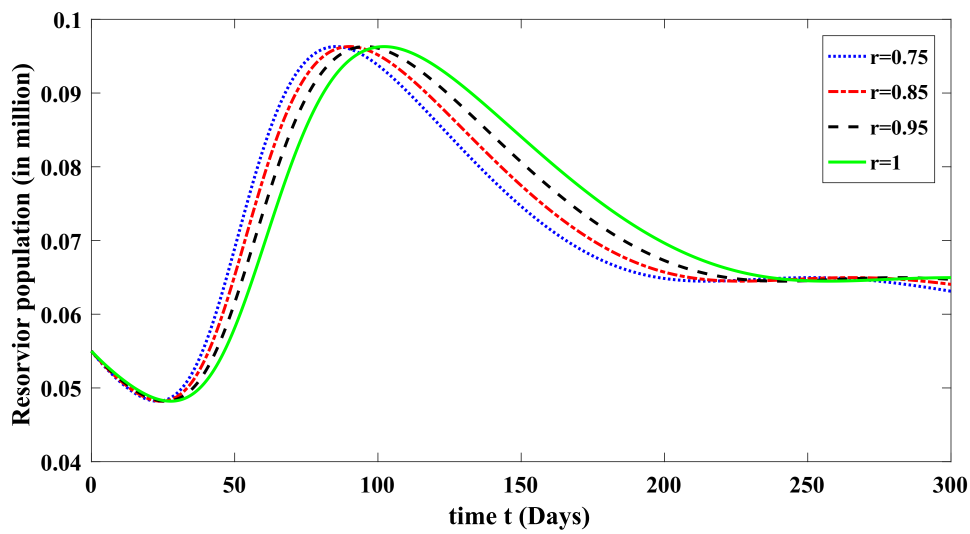

Fig. 6 Behavior of reservoir population $M(t)$ at various arbitrary order r of the proposed system (2) for $h = 0.1, b_p = 0.05$

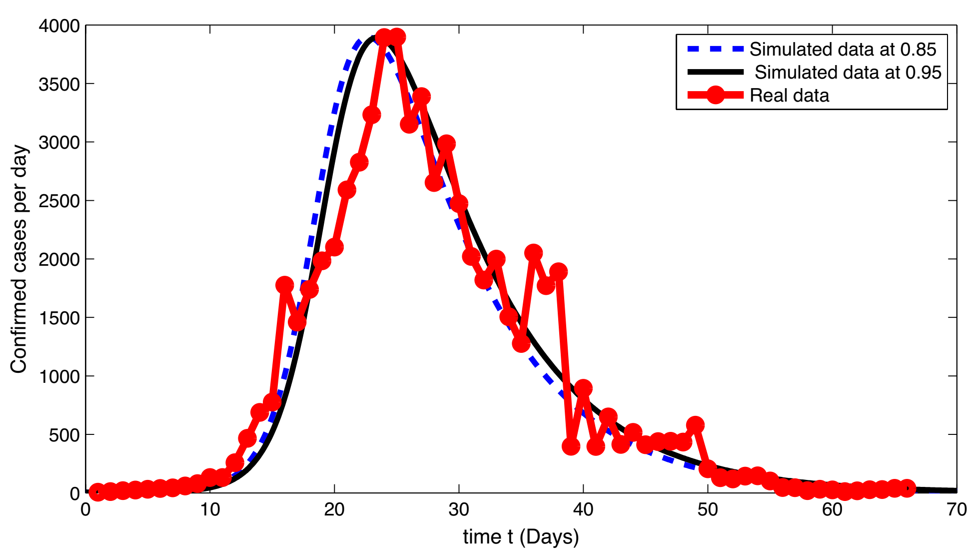

Fig. 7 Behavior of all populations at various arbitrary order r of the proposed system (2) for $h = 0.05, b_p = 0.5$

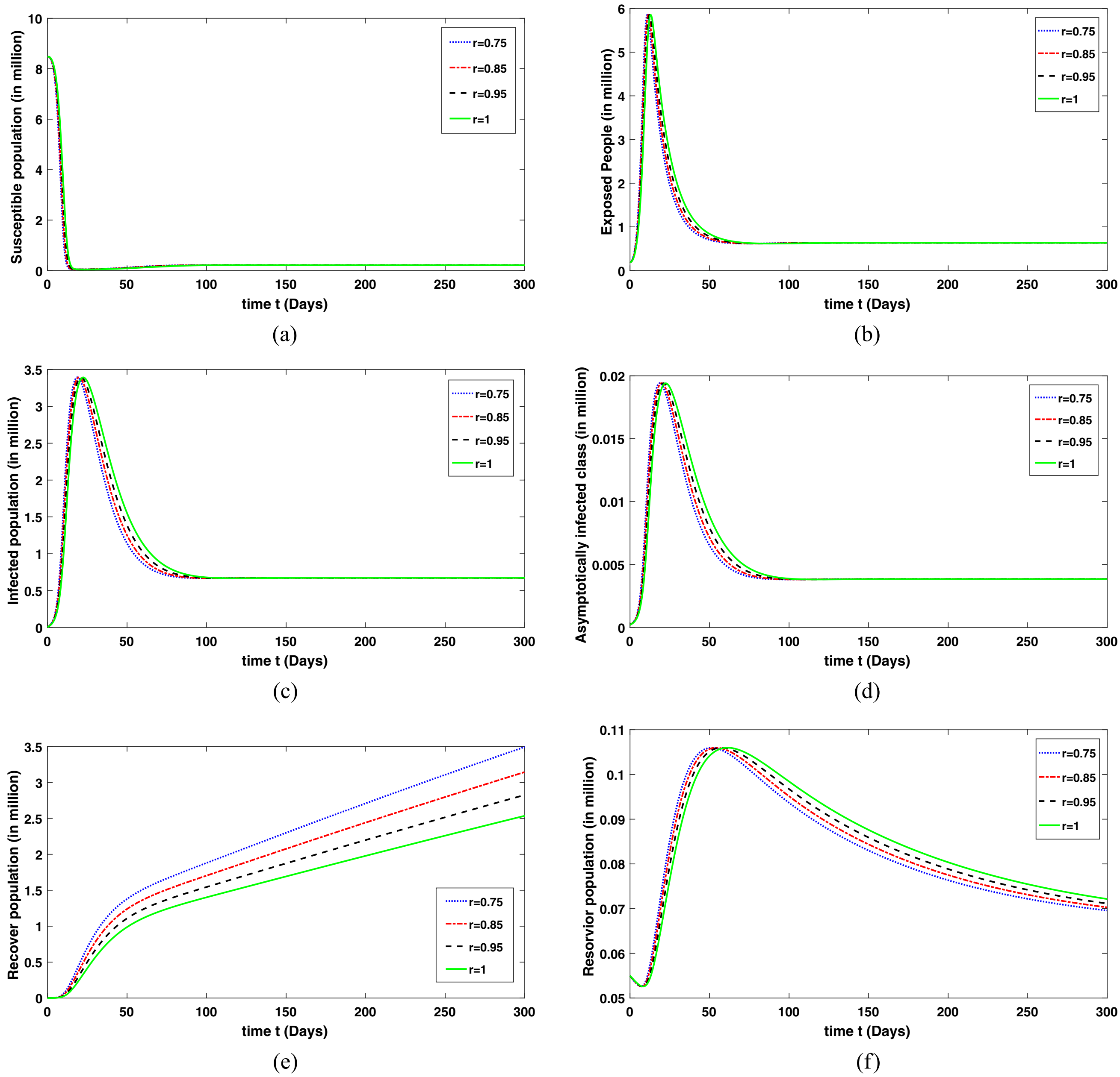

Fig. 8 Behavior of all populations at various arbitrary order r of the proposed system (2) for $h = 0.01, b_p = 0.1$

$$\begin{aligned}R_p(t_{i+1}) = {} & R_p(0) + \tfrac{(1-r)}{ABC(r)}\Big[\mathrm{F}_5(R_p(t_i), t_i)\Big] \\ & + \tfrac{r}{ABC(r)} \sum_{q=0}^{i} \Bigg(\tfrac{F_5(R_p(t_q),t_q)}{\Gamma(r+2)} \Delta^r \Big[(i+1-q)^r(i-q+2+r) \\ & -(i-q)^r(i-q+2+2r)\Big] \\ & - \tfrac{F_5(R_p(t_{q-1}),t_{q-1})}{\Gamma(r+2)} \Delta^r[(i+1-q)^{r+1} - (i-q)^r(i-q+1+r)]\Bigg).\end{aligned}$$

$$\begin{aligned}M(t_{i+1}) = {} & M(0) + \tfrac{(1-r)}{ABC(r)}\Big[\mathrm{F}_6(M(t_i), t_i)\Big] \\ & + \tfrac{r}{ABC(r)} \sum_{q=0}^{i} \Bigg(\tfrac{F_6(M(t_q),t_q)}{\Gamma(r+2)} \Delta^r \Big[(i+1-q)^r(i-q+2+r) \\ & -(i-q)^r(i-q+2+2r)\Big] \\ & - \tfrac{F_6(M(t_{q-1}),t_{q-1})}{\Gamma(r+2)} \Delta^r[(i+1-q)^{r+1} - (i-q)^r(i-q+1+r)]\Bigg).\end{aligned}$$

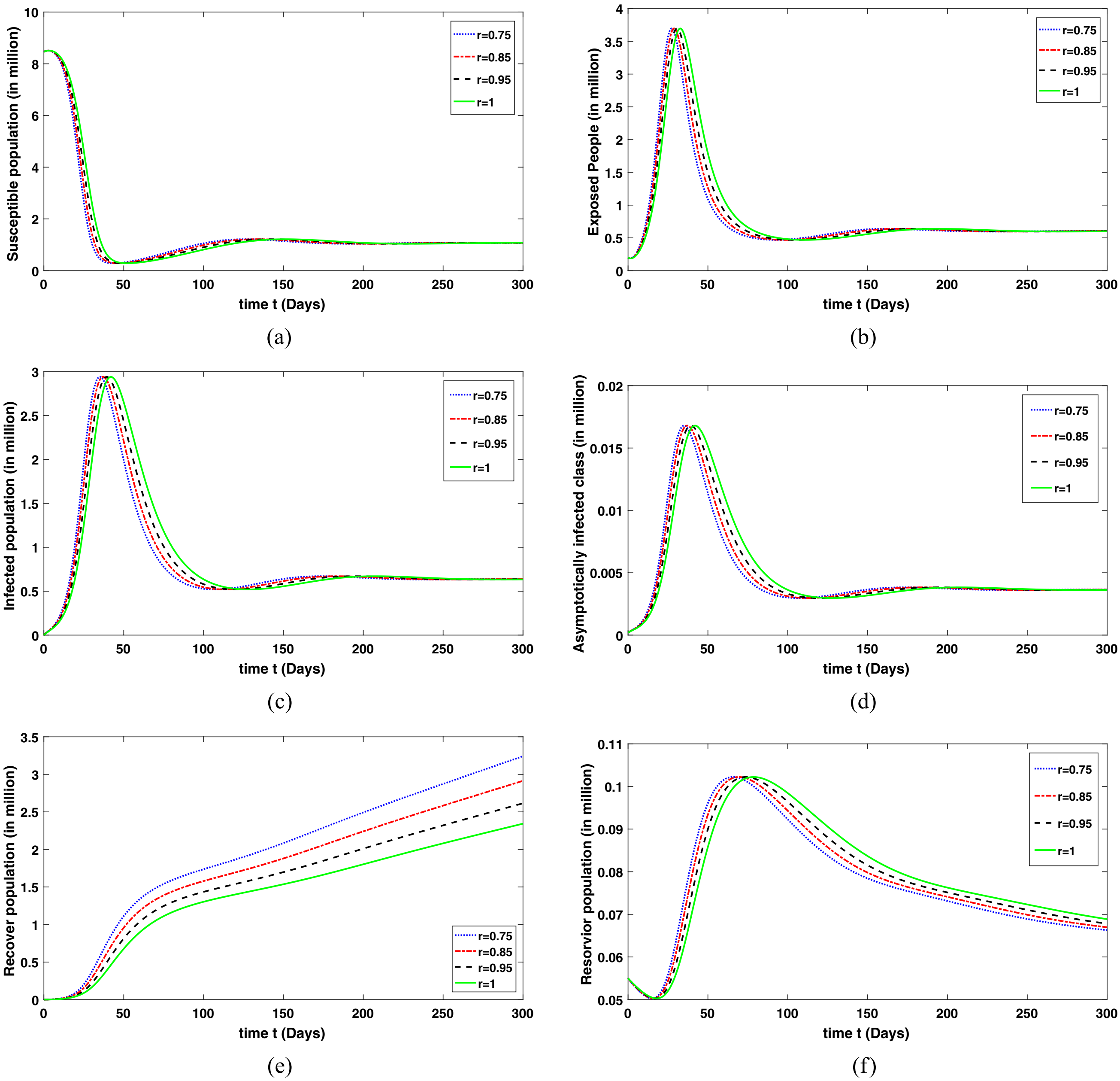

Fig. 9 Comparison between real and simulated data at given different fractional orders for our proposed model

We apply the above procedure to simulate the proposed model in the next section.

4 Experimental results and discussion

The numerical simulation is obtained from the results using data given in Table 2, from [51] with some updating assuming data. Further, the initial data are in million, we have taken in percentage as $S_p(0) = 8.465518$, $E_p(0) = 0.2$, $I_p(0) = 0.0002$, $A_p(0) = 0.0002$, $R_p(0) = 0.0002$, $M(0) = 0.055$, and the values of parameters are given in Table 2.

From Fig. 1, it is observed that increasing rate of transmission will decrease the number of susceptible individuals, and in return, it will increase number of infected population. In other words isolation and keeping social distance will greatly help in controlling the current outbreak for further spreading. The decrease of susceptible has been shown on different fractional order. The order of derivatives has also produced certain impact on the process, initially at smaller order the process of decay is faster than the higher order

Table 3 Description of the parameters given in model (1) for Pakistan

Notation	Numerical value
n_P	0.4673
m_p	0.018
b_p	0.083
b_w	0.000001231
ω_p, ω'_p	0.1243, 0.005
HCode γ_p, γ'_p	0.09871, 0.854302
ε, σ	0.1243, 0.01
ϑ	0.398
δ_p,	0.1243
κ	0.02

and vice versa. After 60 days the susceptible population decreases and then going towards convergency and stability.

From Fig. 2, we conclude that initially the number of exposed individuals is growing up to 50 days for about all orders of derivatives. After that the number decreases gradually, but at this time the decrease occurs differently at different order of derivative. It means that exposed population increases as the symptoms is recognized initially, when the outbreak of pandemic starts. After 40 or 45 days the exposed class begins to decay and then become constant or stable

From Fig. 3, we see that at the given data the number of infected cases are less than that of susceptible and exposed ones. Here up to 50 days the rate of increase is very high and same for all about orders of derivatives, but after that as the transmission of people from place to place decreases the infection is decreasing. The concerned increase and decrease in population are different due to different fractional orders. The infection reached to the peak value on 50^{th} day and then decays to some certain value of 10 infected cases per day, showing stability or convergency.

From Fig. 4, we conclude that initially the asymptotic infected population slightly increases up to 50 days, as the number of infected individuals at this stage is on peak. After that the number decreases gradually or very slowly at different orders of derivative. The number of this class after the 100^{th} day shows stability and became constant. As decrease and increase in this class are very very low or small as compared to other classes, therefore it is known as asymptotic class.

Figure 5 shows that the recovery from disease at the beginning is low as the numbers of infected and exposed are very low. But after some protective actions and precautionary measures, the number of recovered population increases. Here, the recovered population is different for different order of derivatives up to 300 days. After that the increases that occur in the recovered case are different at different fractional order.

Figure 6 demonstrates that the number of reservoir population decreases up to 35 days at different fractional order. After that the number of this class increases as compared to other classes with the passage of time. This means that as no precautionary actions are taken in the society more people will be infected but they will be unaware of their infection which will become cause or reservoir for infection in the future. It means that large number of population will be reserved (infection lies in their bodies) but with the passage of time it is also controlled.

Furthermore, to check the sensitivity of the fractional order model by changing the values of contact rate b_p and step size h in Fig. 7a–f.

Another set has been given from Fig. 8a–f by taking $h = 0.01, b_p = 0.1$.

Here in Fig. 9, we have compared the reported real data [58] of infected cases in Wuhan city from 4th January 2020 to 8th March 2020 for 67 days as [6,12,19,25,31,38,44,60,80,131,131,259,467,688,776,1776,1460,1739,1984,2101,2590,2827,3233,3892,3697,3151,3387,2653,2984,2473,2022,1820,1998,1506,1278,2051,1772,1891,399,894,397,650,415,518,412,439,441,435,579,206,130,120,143,146,102,46,45,20,31,26,11,18,27,29,39,39]

We see that the simulated data has close agreement with the plot of the real data. This phenomenon demonstrates the efficiency of our numerical results (Fig. 10).

Next we use the second data for Pakistan as in [59]. The initial population is $S_p(0) = 220$, $E_p(0) = 120, I_p(0) = 1.30$, $A_p(0) = 0.3$, $R_p(0) = 1.02$, $M(0) = 1.055$. The parameters values are given in Table 2 [59] (Table 3).

Hence present comparison between real data and simulated data Fig. 11. The confirmed cases in Pakistan per day reported in [60] from the 1 March 2021 to 15th of September 2021 for 200 days as [4,4,5,5,5,5,5,6,15,17,18,19,19,31,51,182,245,331,439,485,629,758,856,962,1034,1171,1139,1454,1554,1836,19972262,2520,2646,2899,3058,3549,3735,3852,3902,4162,4150,4307,4362,4824,5143,5122,5660,6043,6742,7286,7703,8479,8925,9438,10103,10586,11058,11747,11996,12380,12900,13818,14498,14814,15716,16370,17574,18003,20267,21587,22037,23268,25609,26003,26230,27054,27904,29266,30503,31775,32578,34386,34642,36228,37657,38150,38900,39690,40358,40880,42687,44777,47607,50234,53300,56144,59394,63400,57170,60470,75053,78699,83182,79700,84762,85321,89583,93233,97690,100324,104648,105087,106142,107733,107270,107607,107460,107784,106023,106775,106361,108100,108466,103543,95388,95241,95219,94522,91408,90358,89250,87345,86770,84234,77418,77360,73536,60234,57668,53431,53333,52203,51057,50080,40242,29274,29626,27189,26191,25279,24983,24941,24912,24908,24935,24827,20597,19230,18253,17573,17548,17555,17588,17103,16229,16685,16014,16001,13706,13385,12464,11697,11542,10378,10446,9940,9356,8739,8555,8585,8500,8553,8623,8633,8564,8512,8660,8883,6020,6234,6477,6545,5291,5546,5979,5786,5582,5525]

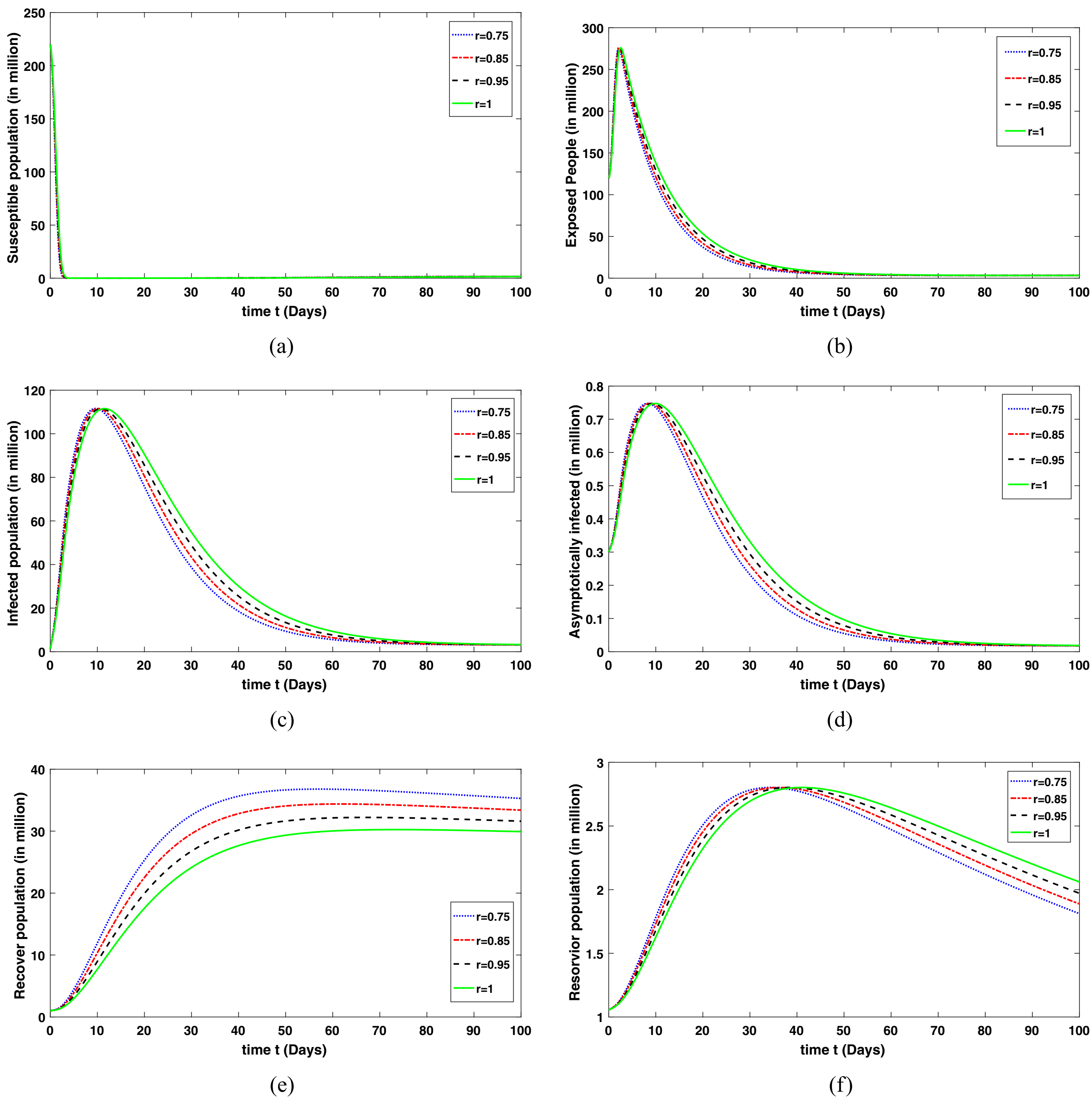

Fig. 10 Behavior of all populations at various arbitrary order r of the proposed system (2) for $h = 0.01$

5 Concluding remarks

Assigning different experimental values taken from [51, 59] to the parameters of (2), we have performed the required simulations as compared to integer order simulation of the system (1). We noticed that by increasing rate of protection, cure and decrease rate of transmission, the minimization and stabling in the numbers of infected individuals can be achieved. By studying such dynamical system, one can know how to control the population from being infected and isolation of infected ones from transmission (immigration). This will be very easy for policy makers and health sector to implement precautionary measures. We can predict for future on the basis of basic reproductive number. From epidemiological point of view it will be very interesting for medical science researchers to know about the history (past), present and future of infection by investigating such type of fractional mathematical model for the pandemic. This model can be applied to the population where social gathering occurs locally or globally. Further, by using fixed point theory the solution of the considered fractional dynamical system has been proved for the existence and uniqueness, while the rate of decaying and growth has been shown through global ways.

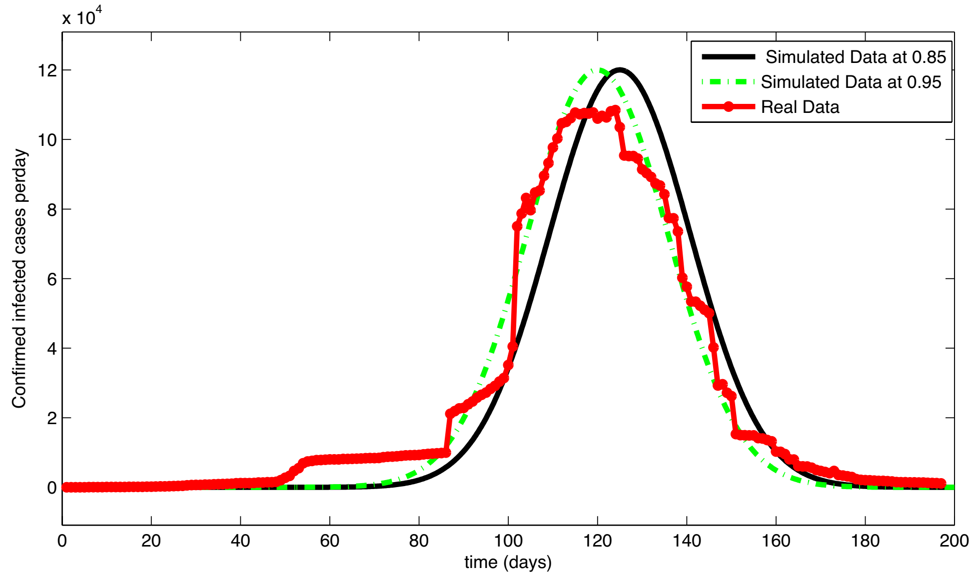

Fig. 11 Comparison between real and simulated data at given different fractional orders for our proposed model

Hence, fractional calculus can be used for comprehensive explanation of various dynamical models. Further, we observe that increasing precautionary measures will increase the recovered population. The data of Wuhan and Pakistan have been used to demonstrate the model. Also we have compared our simulated data with some reported real data of Wuhan and Pakistan for infected population. We have observed that both simulated and real data plots closely agreed. This shows that the established results are true and applicable. These types of models usually provide interesting indications for future planning and understanding the transmission dynamics of the disease.

Acknowledgements This research was funded by the Princess Nourah bint Abdulrahman University Researchers Supporting Project number (PNURSP2022R152), Princess Nourah bint Abdulrahman University, Riyadh, Saudi Arabia. Authors Kamal Shah and Thabet Abdeljawad would like to thank Prince Sultan University for the support through research Lab TAS.

Funding This research was funded by the Princess Nourah bint Abdulrahman University Researchers Supporting Project number (PNURSP2022R152), Princess Nourah bint Abdulrahman University, Riyadh, Saudi Arabia.

Declarations

Conflict of interest The authors declare no competing interests.

References

1. Is the World Ready for the Coronavirus. Editorial, The New York Times, 29 January 2020, Archived from the original on 30 January 2020
2. China virus death toll rises to 41, more than 1,300 infected worldwide, CNBC, 24 January 2020. Archived from the original on 26 January 2020. Retrieved 26 January 2020. Retrieved 30 January 2020
3. Zhai P, Ding Y, Wu X, Long J, Zhong Y, Li Y (2020) The epidemiology, diagnosis and treatment of COVID-19. Int J Antimicrob Agents 55(5):105955
4. Chowdhury SD, Oommen AM (2020) Epidemiology of COVID-19. J Dig Endosc 11(01):03–07
5. Lipsitch M, Swerdlow DL, Finelli L (2020) Defining the epidemiology of Covid-19-studies needed. N Engl J Med 382(13):1194–1196
6. Tyrrell DA, Bynoe ML (1966) Cultivation of viruses from a high proportion ofpatients with colds. Lancet 1:76–77
7. Kahn JS, McIntosh K (2005) History and recent advances in coronavirus discovery. Pediatr Infect Dis J 24(11):223–227
8. Lu H, Stratton CW, Tang YW (2020) Outbreak of pneumonia of unknown etiology in Wuhan, China: The mystery and the miracle. J Med Virol 92(4):401
9. Goyal M, Baskonus HM, Prakash A (2019) An efficient technique for a time fractional model of lassa hemorrhagic fever spreading in pregnant women. Eur Phys J Plus 134(481):1–10
10. Gao W, Veeresha P, Prakasha DG, Baskonus HM, Yel G (2020) New approach for the model describing the deathly disease in pregnant women using Mittag-Leffler function. Chaos Solit Fractals 134:109696
11. Kumar D, Singh J, Al-Qurashi M, Baleanu D (2019) A new fractional SIRS-SI malaria disease model with application of vaccines, anti-malarial drugs, and spraying. Adv Differ Equ 278:1–10
12. Shah K, Alqudah MA, Jarad F, Abdeljawad T (2020) Semi-analytical study of Pine Wilt Disease model with convex rate under Caputo-Febrizio fractional order derivative. Chaos Solitons Fractals 135:109754
13. Shahid A, Huang HL, Khalique CM, Bhatti MM (2021) Numerical analysis of activation energy on mhd nanofluid flow with exponential temperature-dependent viscosity past a porous plate. J Therm Anal Calorim 143(3):2585–2596
14. Zhang L, Bhatti MM, Marin M, Mekheimer KhS (2020) Entropy analysis on the blood flow through anisotropically tapered arteries filled with magnetic zinc-oxide (zno) nanoparticles. Entropy 22(10):1070
15. Bhatti MM, Alamri SZ, Ellahi R, Abdelsalam S (2020) Intrauterine particle-fluid motion through a compliant asymmetric tapered channel with heat transfer. J Ther Anal Calor 21:1–9

16. Shi Z et al (2020) Estimating the serial interval of the novel coronavirus disease (COVID-19): a statistical analysis using the public data in Hong Kong from January 16 to February 15, 2020. Frontiers in Physics 8:347
17. Zhao SS et al (2020) Preliminary estimation of the basic reproduction number of novel coronavirus (2019-nCoV) in China, from 2019 to 2020: a data-driven analysis in the early phase of the outbreak. Int J Infect Dis 92:214–217
18. Riou J, Althaus CL (2020) Pattern of early human-to-human transmission of Wuhan 2019 novel coronavirus (2019-nCoV), December 2019 to January 2020. Eurosurveillance 25(4):2000058
19. Li X et al (2020) Transmission dynamics and evolutionary history of 2019-nCoV. J Med Virology 92(5):501–511
20. Mahase E (2020) Coronavirus: UK screens direct flights from Wuhan after US case, B. Med J 368:m265
21. Li QQ et al (2020) Early transmission dynamics in Wuhan, China, of novel Coronavirus-infected pneumonia. N Engl J Med 382:1199–1207
22. Zhang X (2020) Epidemiology of COVID-19. N Engl J Med 382(19):1869
23. Podlubny I (1999) Fractional Differential Equations, Mathematics in Science and Engineering. Academic Press, New York
24. Lakshmikantham V, Leela S, Vasundhara J (2009) Theory of Fractional Dynamic Systems. Cambridge Academic Publishers, Cambridge, UK
25. Hilfer R (2000) Applications of Fractional Calculus in Physics. World Scientific, Singapore
26. Rossikhin YA, Shitikova MV (1997) Applications of fractional calculus to dynamic problems of linear and nonlinear hereditary mechanics of solids. Appl Mech Rev 50:15–67
27. Kilbas AA, Marichev OI, Samko SG (1993) Fractional Integrals and Derivatives (Theory and Applications). Gordon and Breach, Switzerland
28. Toledo-Hernandez R, Rico-Ramirez V, Iglesias-Silva GA, Diwekar UM (2014) A fractional calculus approach to the dynamic optimization of biological reactive systems. Part I: Fractional models for biological reactions. Chemecal Engineering Science 117:217–228
29. Miller KS, Ross B (1993) An Introduction to the Fractional Calculus and Fractional Differential Equations. Wiley, New York
30. Kilbas AA, Srivastava H, Trujillo J (1996) Theory and Application of Fractional Differential Equations North Holland Mathematics Studies, vol 204. Elseveir, Amsterdam
31. Shah K, Jarad F, Abdeljawad T (2020) On a nonlinear fractional order model of dengue fever disease under Caputo-Fabrizio derivative. Alex Eng J 59(4):2305–2313
32. Biazar J (2006) Solution of the epidemic model by Adomian decomposition method. Appl Math Comput 173:1101–1106
33. Rafei M, Ganji DD, Daniali H (2007) Solution of the epidemic model by homotopy perturbation method. Appl Math Comput 187:1056–1062
34. Rafei M, Daniali H, Ganji DD (2007) Variational iteration method for solving the epidemic model and the prey and predator problem. Appl Math Comput 186:1701–1709
35. Lin Q et al (2020) A conceptual model for the coronavirus disease 2019 (COVID-19) outbreak in Wuhan, China with individual reaction and governmental action. Int J Infec Diseases 93:211–216
36. Richard K, Wilhelm HD (2016) Numerical Methods and Modelling for Engineering. Springer, New York
37. Naz R, Naeem I (2019) The approximate Noether symmetries and approximate first integrals for the approximate Hamiltonian systems. Nonlinear Dyn 96:2225–2239
38. Al-Refai M, Abdeljawad T (2017) Analysis of the fractional diffusion equations with fractional derivative of non-singular kernel. Advances in Difference Equations, (2017): 315
39. Abdeljawad T (2017) Fractional operators with exponential kernels and a Lyapunov type inequality. Advances in Difference Equations, (2017): 313
40. Shatha H et al (2020) Atangana-Baleanu fractional framework of reproducing kernel technique in solving fractional population dynamics system. Chaos, Solitons Fractals 133:109624
41. Khan SA, Shah K, Jarad F, Zaman G (2019) Existence theory and numerical solutions to smoking model under Caputo-Fabrizio fractional derivative. Chaos 29(1):013128
42. Shah K, Alqudah MA, Jarad F, Abdeljawad T (2020) Semi-analytical study of Pine Wilt Disease model with convex rate under Caputo-Fabrizio fractional order derivative. Chaos, Solitons Fractals 135:109754
43. Haq F, Shah K, Rahman G, Shahzad M (2018) Numerical solution of fractional order smoking model via Laplace Adomian decomposition method. Alex Eng J 57(2):1061–1069
44. Haq F, Shah K, Rahman G, Shahzad M (2017) Numerical analysis of fractional order model of HIV-1 infection of CD4+ T-cells. Comput Method Diff Equ 5(1):1–11
45. Iserles A (1996) A First Course in the Numerical Analysis of Differential Equations. Cambridge University Press
46. Butcher JC (2003) Numerical Methods for Ordinary Differential Equations. John Wiley, New York
47. Naghipour A, Manafian J (2015) Application of the Laplace adomian decomposition method and implicit methods for solving Burger's equation. J Pure Apple Math 6(1):68–77
48. Rida SZ, Abdel Rady AS, Arafa AAM, Khalil M (2012) Approximate analytical solution of the fractional epidemic model. IJMR 1:17–19
49. Brailsford SC et al (2009) An analysis of the academic literature on simulation and modelling in health care. J Simul 3(3):130–140
50. Rappaz J, Touzani R (1992) On a two-dimensional magnetohydrodynamic problem: modelling and analysis. Math Model Numer Anal 26(2):347–364
51. Veeresha P et al (2020) Novel dynamical structures of COVID-19 with nonlocal operator via new computational technique. Biology 9(5):107
52. Khan MA, Atangana A (2020) Modeling the dynamics of novel coronavirus (2019-nCov) with fractional derivative. Alexandria Eng J 59(4):2379–2389
53. Porwal P, Shrivastava P, Tiwari SK (2015) Study of simple SIR epidemic model. Adv Appl Sci Res 6(4):1–4
54. Abdeljawad T, Baleanu D (2016) Discrete fractional differences with nonsingular discrete Mittag-Leffler kernels. Adv Difference Equ 1:1–18
55. Burton TA (2019) Krasnoselskii N-tupled fixed point theorem with applications to fractional nonlinear dynamical system, Advances in Mathematical Physics 2019, Article ID 6763842 9 pages
56. Gómez JF et al (2019) Fractional Derivatives with Mittag-Leffler Kernel. Springer
57. Richardson BC (1979) Limitations on the use of mathematical models in transportation policy analysis, University Microfilms International. Ann Arbor, Mich
58. COVID-19 Coronavirus Pandemic, https://www.worldometers.info/coronavirus/reprot, Accessed March 26, 2020
59. https://www.worldometers.info/world-population/pakistan-population/ 25 January 2022
60. https://covid.gov.pk/ Situation of covid-19 in Pakistan from March 2021 to September 2021

Muhammad Arfan is working as lecturer for 8 years in government degree college gulabad Dir lower KPK Pakistan. Also PhD scholar in the department t of mathematics at University of Malakand Dir Lower KPK Pakistan.

Maha M. A. Lashin received the Ph.D. degree in artificial intelligent from Cairo University, Egypt. She is currently an Associate Professor in mechanical design and production with the College of Engineering, Princess Nourah Bint Abdulrahman University (PNU), Saudi Arabia, and a Supervisor of master's and Philosophy Doctor degrees for students of engineering colleges, such as smart memory alloy development for the effective use of control systems, diagnosis of machinery malfunctions by analyzing the vibrations using genetic algorithms, modeling and simulation of the static and dynamic performance of sandwich beams, and control of air handling unit as a method of reducing power consuming.

Pongsakorn Sunthrayuth is a Lecturer at Rajamangala University of Technology Thanyaburi in Applied mathematics. His research interests are Variational Inequalities, Fixed Point Theory, Iterative Methods, Mathematical Analysis, Applied Analysis, Differential Equations, Convex Optimization, Nonlinear Optimization, Multiobjective Optimization, and Mathematical Programming.

Kamal Shah Shah is a senior researcher in the Department of Mathematics & Sciences, Prince Sultan University, Riyadh, Saudi Arabia. From 2007 to 2021, he was an associate professor in the Department of Mathematics, University of Malakand, Chakdara, Pakistan. He obtained a master's in Mathematics from Government Post Graduate Jahanzeb College, Swat, Pakistan, in 2005. He joined the University of Malakand as a lecturer in 2007 and obtained his Ph.D. in Fractional Calculus in 2016 from the same university.

Aman Ullah is working as Assistant Professor (from 10-04-2012 to Date), Department of Mathematics, University of Malakand, Chakdara, Dir Lower, KPK, Pakistan. He worked as a Lecturer (from 01-10-2004 to 09-04-2012), Department of Mathematics, University of Malakand, Chakdara, Dir Lower, KPK, Pakistan. He also worked as a Lecture in GPGJ College Saidu Sharif Swat(from Oct 2002 to Oct 2003).

Kulpash Iskakova is Professor at The National Pedagogical University. Her research interests are Materials Physics, Computational Physics, Condensed Matter Physics, Artificial Neural Network, Artificial Intelligence, Computing in Mathematics, Natural Science, and Engineering and Medicine.

M. R. Gorji is a senior researcher at Ghent University, Belgium. His research interests are Biomedical Engineering, Fluid Mechanics, Computational Fluid Dynamics, Heat Transfer, Drug Delivery, Nanofluilds, Renewable Energy, and Mathematical Modeling.

Thabet Abdeljawad received the Ph.D. degree in mathematics from Middle East Technical University, in 2000. He is currently a Full Professor with Prince Sultan University. He has published more than 450 research articles in different well-known journals. He has been listed as a highly cited researcher for the three consecutive years 2019, 2020, and 2021. He has published more than 450 research articles in different well-known journals. His main research interests include fractional calculus, discrete fractional operators, metric spaces, and fixed point theory.